Available online at www.sciencedirect.com

ScienceDirect

Chinese Journal of Aeronautics 20(2007) 415-424

Chinese Journal of Aeronautics

www.elsevier.com/locate/cja

Large Amplitude Flexural Vibration of the Orthotropic Composite Plate Embedded with Shape Memory Alloy Fibers

Ren Yongsheng[a,*], Sun Shuangshuang[b]

[a]*College of Mechanical and Electronic Engineering, Shandong University of Science and Technology, Qingdao 266510 , China*

[b]*School of Electro-mechanical Engineering, Qingdao University of Science and Technology, Qingdao 266061 , China*

Received 22 January 2007; accepted 4 July 2007

Abstract

The free and forced vibration of large deformation composite plate embedded with shape memory alloy (SMA) fibers is investigated. A thermo-mechanical constitutive equation of SMA proposed by Brinson et al. is employed and the constitutive equations for evaluation of the properties of a hybrid SMA composite laminate are obtained. Based on the nonlinear theory of symmetrically laminated anisotropic plates, the governing equations of flexural vibration in terms of displacement and stress functions are derived. The Galerkin method has been used to convert the original partial differential equation into a nonlinear ordinary differential equation, which is then solved with harmonic balance method. The numerical results show that the relationship between nonlinear natural frequency ratio and temperature for the nonlinear plate has similar characteristics compared with that of the linear one, and the effects of temperature on forced response behavior during phase transformation from Martensite to Austenite are significant. The effects of the volume fraction of the SMA fiber, aspect ratio and free vibration amplitude on the dynamical behavior of the plate are also discussed.

Keywords: smart materials; large-deflection plate; composite; nonlinear vibration

1 Introduction

In recent ten years, great progress has been made on the research of shape memory alloy (SMA) reinforced smart structure systems. Through the design of SMA intelligent composite structure systems with highly integrated sensors and actuators, the control of complex flexible structures with rigorous weight limitations such as aeronautic structures has become possible. For example, the buckling and vibration characteristics of SMA reinforced composite plate and beam structures have been greatly improved when compared to traditional composite structures, this makes SMA be widely used in buckling and vibration control[1-2].

For the structures with high strength and large flexibility used in aircraft design, the geometric nonlinear effect resulted from large deformation cannot be ignored. For instance, the shapes of the panels of the supersonic aircraft will be changed due to the large thermal deflections induced by aerodynamic heating, which will affect the aerodynamic characteristics and reduce the flight performance of the aircraft. In order to control such kind of nonlinear structures, it is necessary to know the effect of geometric nonlinearity on the vibration of structures. However, most of the researches on SMA reinforced composite plates and beams are based on the classic small deflection theory and only a few are concerning with the large deflection nonlinearity issues.

*Corresponding author. Tel.: +86-532-88032695.
E-mail address: renys@sdust.edu.cn

Based on von Karman plate theory, Chu L C[3] established the nonlinear finite element model for the SMA fiber reinforced composite large-deflection plate and studied the suppression of the flutter of panels of aircraft. Zou Jing[4] derived the incremental finite element motion equation for the nonlinear composite laminate embedded with SMA fibers on the basis of the virtual work principle, and the bending, thermo-buckling and post-buckling issues of the SMA reinforced composite laminate under transverse loading were discussed. Dano M L et al.[5] studied the effect of SMA on the snap-through characteristics of the nonlinear unsymmetric fiber-reinforced composite laminate with large-deflections. They established the approximate theory to analyze the snap-through characteristics of the unsymmetric fiber-reinforced composite laminate activated by SMA wires, where the mechanical properties of the laminate are predicted with the assumed strain-displacement field, Rayleigh-Ritz method and the virtual work principle, and the law of snap-through varying with the temperature was obtained through solving relevant simultaneous equations and the equation describing SMA properties. Park J S et al.[6-7] established the finite element model of composite laminates and supersonic plates under nonlinear vibration and nonlinear flutter by using the von Karman plate theory, the one-order shearing deformation plate theory and the first-order piston theory. The boundary problems of thermo-post-buckling nonlinear vibration and flutter were then investigated for the SMA fiber reinforced composite plate under thermal and aerodynamic loading. Cho M et al.[8] studied the deformation of the nonlinear composite plate with two-way shape memory effect with the theory of the one-order shearing deformation plate with large deflections and the thermo-mechanical constitutive equation proposed by Lagoudas et al.

Based on the above literature review, we realize that: ① most of the current researches on the geometric nonlinearity of the SMA fiber (or layer) reinforced composite plate are limited to using the finite element numerical method[3-7], and little work has been reported to use the nonlinear elastic theory to get the analytical vibration solution for the SMA reinforced nonlinear anisotropic laminates; ② about the description of the mechanical behavior of SMA, some are based on the expression of the approximate experimental fitting[3], the others use the approximate data derived from the curves of SMA[6-7], and the well-developed and practical constitutive equation of SMA based on the phenomenal theory such as Brinson's equation[4,9] is hardly used; ③ the effect of SMA fibers on the nonlinear vibration of composite plates still needs to be investigated further.

In this paper, the free and forced vibration of the SMA reinforced composite laminates with large deflections will be studied. The thermo-mechanical constitutive equation of SMA proposed by Brinson et al.[4] and the mixture theory for evaluating the properties of laminates are employed to establish the constitutive equation of the SMA reinforced composite laminates with large deflections. Based on the nonlinear theory of symmetrically laminated anisotropic plates, the transverse vibration equation and the compatible equation will be derived in terms of the transverse deflection and the stress function. The Galerkin approximate method and the harmonic balance method (HBM) will be used to solve the Duffing's differential equation and to study the effect of the content of SMA fibers, the nonlinear vibration amplitude and the excitation force amplitude on the natural frequency and steady-state response of the system.

2 Basic Theories

2.1 The constitutive equation of the anisotropic laminate with embedded SMA fibers

As the SMA reinforced anisotropic lamina has the following off-axis stress-strain relation[10]

$$\begin{Bmatrix}\sigma_x\\ \sigma_y\\ \tau_{xy}\end{Bmatrix}=\bar{\boldsymbol{Q}}_{ij}^{(k)}\begin{Bmatrix}\varepsilon_x\\ \varepsilon_y\\ \gamma_{xy}\end{Bmatrix}-\tilde{\boldsymbol{Q}}_{ij}^{(k)}\begin{Bmatrix}\alpha_x^*\\ \alpha_y^*\\ \alpha_{xy}^*\end{Bmatrix}\Delta T+\begin{Bmatrix}\sigma_{\mathrm{rx}}^*\\ \sigma_{\mathrm{ry}}^*\\ \tau_{\mathrm{rxy}}^*\end{Bmatrix} \quad (1)$$

the constitutive equation of the SMA reinforced laminate can be written as

$$\begin{Bmatrix} \boldsymbol{N} \\ \boldsymbol{M} \end{Bmatrix} = \begin{bmatrix} \boldsymbol{A} & \boldsymbol{B} \\ \boldsymbol{B} & \boldsymbol{D} \end{bmatrix} \begin{Bmatrix} \boldsymbol{\varepsilon}^0 \\ \boldsymbol{\kappa} \end{Bmatrix} - \begin{Bmatrix} \boldsymbol{N}_{\Delta T} \\ \boldsymbol{M}_{\Delta T} \end{Bmatrix} + \begin{Bmatrix} \boldsymbol{N}_{\mathrm{r}} \\ \boldsymbol{M}_{\mathrm{r}} \end{Bmatrix} \tag{2}$$

where $\boldsymbol{\varepsilon}^0$ and $\boldsymbol{\kappa}$ denote the strain vector and the curvature vector of the mid-plane, respectively. The in-plane forces and moments induced by SMA (denoted by the subscript r) and temperature (denoted by the subscript ΔT) are respectively expressed as

$$\left.\begin{aligned} \boldsymbol{N}_{\mathrm{r}} &= \begin{pmatrix} N_{\mathrm{r}x} & N_{\mathrm{r}y} & N_{\mathrm{r}xy} \end{pmatrix}^{\mathrm{T}} = \\ &\quad \int_{-h/2}^{h/2} \begin{pmatrix} \sigma_{\mathrm{r}x}^{(k)} & \sigma_{\mathrm{r}y}^{(k)} & \sigma_{\mathrm{r}xy}^{(k)} \end{pmatrix}^{\mathrm{T}} \mathrm{d}z \\ \boldsymbol{M}_{\mathrm{r}} &= \begin{pmatrix} M_{\mathrm{r}x} & M_{\mathrm{r}y} & M_{\mathrm{r}xy} \end{pmatrix}^{\mathrm{T}} = \\ &\quad \int_{-h/2}^{h/2} \begin{pmatrix} \sigma_{\mathrm{r}x}^{(k)} & \sigma_{\mathrm{r}y}^{(k)} & \sigma_{\mathrm{r}xy}^{(k)} \end{pmatrix}^{\mathrm{T}} z\mathrm{d}z \\ \boldsymbol{N}_{\Delta T} &= \begin{pmatrix} N_{\Delta Tx} & N_{\Delta Ty} & N_{\Delta Txy} \end{pmatrix}^{\mathrm{T}} = \\ &\quad \int_{-h/2}^{h/2} \begin{pmatrix} \sigma_{\Delta Tx}^{(k)} & \sigma_{\Delta Ty}^{(k)} & \sigma_{\Delta Txy}^{(k)} \end{pmatrix}^{\mathrm{T}} \mathrm{d}z \\ \boldsymbol{M}_{\Delta T} &= \begin{pmatrix} M_{\Delta Tx} & M_{\Delta Ty} & M_{\Delta Txy} \end{pmatrix}^{\mathrm{T}} = \\ &\quad \int_{-h/2}^{h/2} \begin{pmatrix} \sigma_{\Delta Tx}^{(k)} & \sigma_{\Delta Ty}^{(k)} & \sigma_{\Delta Txy}^{(k)} \end{pmatrix}^{\mathrm{T}} z\mathrm{d}z \end{aligned}\right\} \tag{3}$$

The $\boldsymbol{A}$, $\boldsymbol{B}$ and $\boldsymbol{D}$ in Eq.(2) are expressed as

$$\boldsymbol{A} = \begin{bmatrix} A_{11} & A_{12} & A_{16} \\ A_{12} & A_{22} & A_{26} \\ A_{16} & A_{26} & A_{66} \end{bmatrix}, \boldsymbol{B} = \begin{bmatrix} B_{11} & B_{12} & B_{16} \\ B_{12} & B_{22} & B_{26} \\ B_{16} & B_{26} & B_{66} \end{bmatrix}$$

$$\boldsymbol{D} = \begin{bmatrix} D_{11} & D_{12} & D_{16} \\ D_{12} & D_{22} & D_{26} \\ D_{16} & D_{26} & D_{66} \end{bmatrix} \tag{4}$$

where each element in Eq.(4) is defined as

$$\left(A_{ij}, B_{ij}, D_{ij}\right) = \int_{-h/2}^{h/2} Q_{ij}\left(1, z, z^2\right)\mathrm{d}z \tag{5}$$

where Q_{ij} represents the off-axis elastic constants of the SMA fiber hybrid lamina.

The recovery stresses of SMA and the stresses induced by temperature of the k lamina after coordinate transformation have the following form, respectively.

$$\left.\begin{aligned} \begin{Bmatrix} \sigma_{\mathrm{r}x} \\ \sigma_{\mathrm{r}y} \\ \sigma_{\mathrm{r}xy} \end{Bmatrix}^{(k)} &= \begin{bmatrix} m^2 & n^2 & -2mn \\ n^2 & m^2 & 2mn \\ mn & -mn & m^2-n^2 \end{bmatrix} \begin{Bmatrix} \sigma_{\mathrm{r}} V_{\mathrm{s}} \\ 0 \\ 0 \end{Bmatrix} \\ \begin{Bmatrix} \sigma_{\Delta Tx} \\ \sigma_{\Delta Ty} \\ \sigma_{\Delta Txy} \end{Bmatrix}^{(k)} &= \begin{bmatrix} \bar{\bar{Q}}_{11} & \bar{\bar{Q}}_{12} & \bar{\bar{Q}}_{16} \\ \bar{\bar{Q}}_{21} & \bar{\bar{Q}}_{22} & \bar{\bar{Q}}_{26} \\ \bar{\bar{Q}}_{61} & \bar{\bar{Q}}_{62} & \bar{\bar{Q}}_{66} \end{bmatrix} \begin{Bmatrix} m^2\alpha_1 + n^2\alpha_2 \\ n^2\alpha_1 + m^2\alpha_2 \\ 2mn(\alpha_1 - \alpha_2) \end{Bmatrix} \Delta T \end{aligned}\right\} \tag{6}$$

where $\bar{\bar{Q}}_{ij}$ (i = 1, 2, 6; j = 1, 2, 6) denotes the elastic constant of the composite medium. m and n are the cosine and sine functions of the ply angle in each lamina, respectively.

From Eq.(2), we have

$$\boldsymbol{M} = \boldsymbol{B}\boldsymbol{\varepsilon}^0 + \boldsymbol{D}\boldsymbol{\kappa} - \boldsymbol{M}_{\Delta T} + \boldsymbol{M}_{\mathrm{r}} \tag{7}$$

$$\boldsymbol{\varepsilon}^0 = \boldsymbol{A}^*\boldsymbol{N} + \boldsymbol{B}^*\boldsymbol{\kappa} + \boldsymbol{A}^*(\boldsymbol{N}_{\Delta T} - \boldsymbol{N}_{\mathrm{r}}) \tag{8}$$

where $\boldsymbol{A}^* = \boldsymbol{A}^{-1}$, $\boldsymbol{B}^* = -\boldsymbol{A}^{-1}\boldsymbol{B}$.

Substituting Eq.(8) into Eq.(7), we get

$$\begin{aligned} \boldsymbol{M} &= \boldsymbol{B}\left[\boldsymbol{A}^*\boldsymbol{N} + \boldsymbol{B}^*\boldsymbol{\kappa} + \boldsymbol{A}^*(\boldsymbol{N}_{\Delta T} - \boldsymbol{N}_{\mathrm{r}})\right] + \\ &\quad \boldsymbol{D}\boldsymbol{\kappa} - \boldsymbol{M}_{\Delta T} + \boldsymbol{M}_{\mathrm{r}} = \boldsymbol{B}\boldsymbol{A}^*\boldsymbol{N} + (\boldsymbol{D} + \boldsymbol{B}\boldsymbol{B}^*)\boldsymbol{\kappa} + \\ &\quad \boldsymbol{B}\boldsymbol{A}^*(\boldsymbol{N}_{\Delta T} - \boldsymbol{N}_{\mathrm{r}}) - \boldsymbol{M}_{\Delta T} + \boldsymbol{M}_{\mathrm{r}} \end{aligned} \tag{9}$$

With the following expression

$$\boldsymbol{B}\boldsymbol{A}^* = \boldsymbol{B}\boldsymbol{A}^{-1} = -(-\boldsymbol{A}^{-1}\boldsymbol{B})^{\mathrm{T}} = -(\boldsymbol{B}^*)^{\mathrm{T}} \tag{10}$$

Eq.(9) can be rewritten as

$$\begin{aligned} \boldsymbol{M} &= -(\boldsymbol{B}^*)^{\mathrm{T}}\boldsymbol{N} - (\boldsymbol{B}^*)^{\mathrm{T}}(\boldsymbol{N}_{\Delta T} - \boldsymbol{N}_{\mathrm{r}}) + \\ &\quad \boldsymbol{D}^*\boldsymbol{\kappa} - \boldsymbol{M}_{\Delta T} + \boldsymbol{M}_{\mathrm{r}} \end{aligned} \tag{11}$$

where $\boldsymbol{D}^* = \boldsymbol{D} - \boldsymbol{B}\boldsymbol{A}^{-1}\boldsymbol{B}$.

By expanding Eq.(8), we have the following expression

$$\begin{aligned} \varepsilon^0 = \begin{Bmatrix} \varepsilon_x^0 \\ \varepsilon_y^0 \\ \varepsilon_{xy}^0 \end{Bmatrix} &= \begin{bmatrix} A_{11}^* & A_{12}^* & A_{16}^* \\ A_{21}^* & A_{22}^* & A_{26}^* \\ A_{61}^* & A_{62}^* & A_{66}^* \end{bmatrix} \bullet \\ &\quad \begin{Bmatrix} N_x \\ N_y \\ N_{xy} \end{Bmatrix} + \begin{bmatrix} B_{11}^* & B_{12}^* & B_{16}^* \\ B_{21}^* & B_{22}^* & B_{26}^* \\ B_{61}^* & B_{62}^* & B_{66}^* \end{bmatrix} \begin{Bmatrix} \kappa_x \\ \kappa_y \\ \kappa_{xy} \end{Bmatrix} + \\ &\quad \begin{bmatrix} A_{11}^* & A_{12}^* & A_{16}^* \\ A_{21}^* & A_{22}^* & A_{26}^* \\ A_{61}^* & A_{62}^* & A_{66}^* \end{bmatrix} \begin{Bmatrix} N_{\Delta Tx} - N_{\mathrm{r}x} \\ N_{\Delta Ty} - N_{\mathrm{r}y} \\ N_{xy} - N_{\mathrm{r}xy} \end{Bmatrix} \end{aligned} \tag{12}$$

where $\kappa_x = -w_{,xx}, \kappa_y = -w_{,yy}, \kappa_{xy} = -2w_{,xy}$; and w is the transverse deflection of the laminate.

2.2 Transverse vibration equations

For convenience, the stress function $\psi(x,y)$ is introduced as a separate variable and the in-plane forces are expressed in terms of $\psi(x,y)$ as

$$N_x = \psi_{,yy},\ N_y = \psi_{,xx},\ N_{xy} = -\psi_{,xy} \tag{13}$$

For the symmetric orthotropic laminate, we have $B_{ij}^* = 0,\ A_{ij}^* = \dfrac{Q_{ij}^*}{h},\ D_{ij}^* = D_{ij} = \dfrac{h^3 Q_{ij}}{12},\ \boldsymbol{M}_{\Delta T} = \boldsymbol{M}_{\mathrm{r}} = 0$ and $\boldsymbol{Q}^* = \boldsymbol{Q}^{-1}$ with the expression of $\boldsymbol{Q}$ as

$$\boldsymbol{Q} = \begin{bmatrix} E_1/\mu & \nu_{12}E_2/\mu & 0 \\ \nu_{21}E_1/\mu & E_2/\mu & 0 \\ 0 & 0 & G_{12} \end{bmatrix} \tag{14}$$

where $\boldsymbol{Q}$ is the matrix consisting of elastic constants of the orthotropic lamina with $\mu = 1-\nu_{12}\nu_{21}$, $\nu_{12}/E_1 = \nu_{21}/E_2$; E_i, ν_{ij} and G_{ij} (i = 1, 2; j = 1, 2) denote the engineering elastic constants of the SMA fiber hybrid composites which are calculated according to the mixture method proposed by Zhong Z W et al.[11] (see appendix A).

According to the characteristics of the symmetric orthotropic laminates, we have the following expressions

$$\left.\begin{aligned} &A_{11}^* = \frac{1}{h}C_{11}^* = \frac{1}{E_1 h} = \frac{\delta_2}{h}, A_{22}^* = \frac{C_{22}^*}{h} = \frac{1}{E_2 h} = \frac{\delta_1}{h} \\ &A_{12}^* = \frac{C_{12}^*}{h} = -\frac{\nu_{12}}{E_1 h},\ A_{66}^* = \frac{C_{66}^*}{h} = \frac{1}{G_{12}h} \\ &2A_{12}^* + A_{66}^* = -\frac{2\nu_{12}}{E_1 h} + \frac{1}{G_{12}h} = \frac{2}{h}\left(\frac{1}{2G_{12}} - \frac{\nu_{12}}{E_1}\right) = \frac{2\delta_3}{h} \end{aligned}\right\} \tag{15}$$

Also, Eq.(8)and Eq.(11) are simplified as

$$\boldsymbol{\varepsilon}^0 = \boldsymbol{A}^*\boldsymbol{N} + \boldsymbol{A}^*(\boldsymbol{N}_{\Delta T} - \boldsymbol{N}_{\mathrm{r}}) \tag{16}$$

$$\boldsymbol{M} = \boldsymbol{D}\boldsymbol{\kappa} \tag{17}$$

Then the transverse vibration equation in terms of the transverse deflection w and the stress function ψ is written as

$$D_1 w_{,xxxx} + 2D_3 w_{,xxyy} + D_2 w_{,yyyy} + \rho w_{,tt} - q - L^*(w,\psi) = 0 \tag{18}$$

where $D_1 = \dfrac{E_1 h^3}{12\mu}$, $D_2 = \dfrac{E_2 h^3}{12\mu}$, $D_3 = \nu_{12}D_2 + 2D_4$, $D_4 = \dfrac{G_{12}h^3}{12}$, ρ and q represent the density and the transverse excitation force of the plate respectively.

The arithmetic operator $L^*(w, \psi)$ in Eq.(18) is expressed as

$$L^*(w,\psi) = w_{,xx}\psi_{,yy} + w_{,yy}\psi_{,xx} - 2w_{,xy}\psi_{,xy} \tag{19}$$

The compatible equation is written as

$$\varepsilon_{x,yy}^0 + \varepsilon_{y,xx}^0 - \varepsilon_{xy,xy}^0 = w_{,xy}^2 - w_{,xx}w_{,yy} \tag{20}$$

Substituting Eq.(16) into Eq.(20) and considering that $\boldsymbol{N}_{\Delta T}$ and $\boldsymbol{N}_{\mathrm{r}}$ are independent of the coordinates, we get the following supplemental equation

$$\delta_1\psi_{,xxxx} + 2\delta_3\psi_{,xxyy} + \delta_2\psi_{,yyyy} + \frac{h}{2}L^*(w,w) = 0 \tag{21}$$

The von Karman's nonlinear strain-displacement relations are

$$\left.\begin{aligned} \varepsilon_x^0 &= u_{,x}^0 + \frac{1}{2}w_{,x}^2 \\ \varepsilon_y^0 &= v_{,y}^0 + \frac{1}{2}w_{,y}^2 \\ \varepsilon_{xy}^0 &= u_{,y}^0 + v_{,x}^0 + w_{,x}w_{,y} \end{aligned}\right\} \tag{22}$$

where u^0, v^0 are in-plane displacements of the plate in x and y directions, respectively.

Replacing the items in the first two equations in Eq.(16) with Eq.(22) and integrating them for x and y, we can obtain the displacements in the midplane. The in-plane displacement boundary conditions can be expressed as

$$\begin{aligned} u^0\big|_{x=a} - u^0\big|_{x=-a} = {} & A_{11}^*\int_{-a}^{a}\psi_{,yy}\mathrm{d}x + A_{12}^*\psi_{,x}\big|_{-a}^{a} - \\ & \frac{1}{2}\int_{-a}^{a}w_{,x}^2\mathrm{d}x + 2a\left[A_{11}^*(N_{\Delta Tx} - N_{\mathrm{r}x}) + \right. \\ & \left. A_{12}^*(N_{\Delta Ty} - N_{\mathrm{r}y})\right] = 0 \end{aligned} \tag{23}$$

$$\begin{aligned} v^0\big|_{y=b} - v^0\big|_{y=-b} = {} & A_{22}^*\int_{-b}^{b}\psi_{,xx}\mathrm{d}y + A_{12}^*\psi_{,y}\big|_{-b}^{b} - \\ & \frac{1}{2}\int_{-b}^{b}w_{,y}^2\mathrm{d}y + 2b\left[A_{12}^*(N_{\Delta Tx} - N_{\mathrm{r}x}) + \right. \\ & \left. A_{22}^*(N_{\Delta Ty} - N_{\mathrm{r}y})\right] = 0 \end{aligned} \tag{24}$$

It should be noted that Eq.(18) and Eq.(21) are the basic equations of the SMA reinforced orthotropic laminates with large deflections in nonlinear vibration, and Eq.(23) and Eq.(24) are the equations with in-plane unmovable constraints.

2.3 Galerkin approximate solution

For the simply-supported plate, one-item approximate solution is taken as

$$w(x,y,t)=hf(t)\cos\frac{\pi x}{2a}\cos\frac{\pi y}{2b} \tag{25}$$

Substituting the above solution into Eq.(21), we have

$$\delta_1\psi_{,xxxx}+2\delta_3\psi_{,xxyy}+\delta_2\psi_{,yyyy}=$$
$$-\frac{1}{2}h^3f^2(t)\left(\frac{\pi}{2a}\right)^2\left(\frac{\pi}{2b}\right)^2(\cos\frac{\pi x}{a}+\cos\frac{\pi y}{b}) \tag{26}$$

Assume the general solution of Eq.(26) is

$$\psi=\psi_{\rm p}+\psi_{\rm c} \tag{27}$$

where, $\psi_{\rm p}$ and $\psi_{\rm c}$ denote the inhomogeneous particular solution and the homogeneous general solution of Eq.(26), respectively. Assume

$$\psi_{\rm p}=C_1\cos\frac{\pi x}{a}+C_2\sin\frac{\pi y}{b} \tag{28}$$

Substituting it into Eq.(26) produces

$$C_1=-\frac{h^2f^2(t)}{32A_{22}^*}\left(\frac{a}{b}\right)^2,\ C_2=-\frac{h^2f^2(t)}{32A_{11}^*}\left(\frac{b}{a}\right)^2 \tag{29}$$

Taking $\psi_{\rm c}$ as

$$\psi_{\rm c}=\frac{1}{2}A_1x^2+\frac{1}{2}A_2y^2 \tag{30}$$

Substituting

$$\psi=\psi_{\rm p}+\psi_{\rm c}=C_1\cos\frac{\pi x}{a}+C_2\sin\frac{\pi y}{b}+\frac{1}{2}A_1x^2+\frac{1}{2}A_2y^2$$

into the displacement boundary conditions Eq.(23) and Eq.(24), we have

$$\left.\begin{aligned}A_1&=\frac{1}{\Delta}\left[\left(\frac{\pi}{2a}\right)^2-\frac{A_{11}^*}{A_{12}^*}\left(\frac{\pi}{2b}\right)^2\right]\frac{h^2}{8A_{12}^*}f^2(t)-N_y\\A_2&=\frac{1}{\Delta}\left[\left(\frac{\pi}{2b}\right)^2-\frac{A_{22}^*}{A_{12}^*}\left(\frac{\pi}{2a}\right)^2\right]\frac{h^2}{8A_{12}^*}f^2(t)-N_x\end{aligned}\right\} \tag{31}$$

where $\Delta=1-\dfrac{A_{11}^*A_{22}^*}{A_{12}^{*2}}$, $N_x=N_{\Delta Tx}-N_{\rm rx}$, $N_y=N_{\Delta Ty}-N_{\rm ry}$.

Using the Galerkin method after substituting Eq.(25) and Eq.(27) into Eq.(18), we get

$$\int_{-a}^{a}\int_{-b}^{b}\Big[D_1w_{,xxxx}+2D_3w_{,xxyy}+D_2w_{,yyyy}+$$
$$\rho w_{,tt}-q-L^*(w,\psi)\Big]\cos\frac{\pi x}{2a}\cos\frac{\pi y}{2b}{\rm d}x{\rm d}y=0 \tag{32}$$

By integrating the above equation and making some simplifications, the nonlinear differential equation with respect to time t is obtained.

$$\rho h\frac{{\rm d}^2f(t)}{{\rm d}t^2}+\left[D_1\left(\frac{\pi}{2a}\right)^4+2D_3\left(\frac{\pi}{2a}\right)^2\left(\frac{\pi}{2b}\right)^2+D_2\left(\frac{\pi}{2b}\right)^4-\left(\frac{\pi}{2a}\right)^2N_x-\left(\frac{\pi}{2b}\right)^2N_y\right]\frac{hf(t)}{4}+$$
$$\frac{h^3f^3(t)}{32}\left\{\left(\frac{\pi}{2a}\right)^2\frac{1}{A_{12}^*\Delta}\left[\left(\frac{\pi}{2b}\right)^2-\frac{A_{22}^*}{A_{12}^*}\left(\frac{\pi}{2a}\right)^2\right]+\left(\frac{\pi}{2b}\right)^2\frac{1}{A_{12}^*\Delta}\left[\left(\frac{\pi}{2a}\right)^2-\frac{A_{11}^*}{A_{12}^*}\left(\frac{\pi}{2b}\right)^2\right]+\frac{\pi^4}{2(2ab)^2}\cdot$$
$$\left[\frac{1}{A_{22}^*}\left(\frac{a}{b}\right)^2+\frac{1}{A_{11}^*}\left(\frac{b}{a}\right)^2\right]\right\}=\frac{4q}{\pi^2}\sin(\omega t+\theta) \tag{33}$$

If some non-dimensional quantities are introduced as below

$$\left.\begin{aligned}\tau&=\left(\frac{E_2h^3}{\rho b^4}\right)^{\frac{1}{2}}t,\ \lambda=\frac{a}{b}\\\bar N_{\rm rx}&=\frac{b^2}{E_2h^3}N_{\rm rx},\ \bar N_{ry}=\frac{b^2}{E_2h^3}N_{\rm ry}\\\bar N_{\Delta Tx}&=\frac{b^2}{E_2h^3}N_{\Delta Tx},\ \bar N_{\Delta Ty}=\frac{b^2}{E_2h^3}N_{\Delta Ty}\\\bar q&=\frac{qb^4}{E_2h^4}\end{aligned}\right\} \tag{34}$$

Eq.(33) will become a non-dimensional equation.

$$\frac{{\rm d}^2f(\tau)}{{\rm d}\tau^2}+\frac{1}{4}\left[\left(\frac{\pi}{2}\right)^4\frac{1}{\lambda^4}\frac{E_1}{12\mu E_2}+2\left(\frac{\pi}{2}\right)^4\frac{1}{\lambda^2}\left(\frac{\nu_{12}}{12\mu}+\frac{1}{6}\frac{G_{12}}{E_2}\right)+\left(\frac{\pi}{2}\right)^4\frac{1}{12\mu}+\left(\frac{\pi}{2}\right)^2\frac{1}{\lambda^2}\left(\bar N_{\rm rx}-\bar N_{\Delta Tx}\right)+\right.$$

$$\left(\frac{\pi}{2}\right)^2\left(\bar{N}_{ry}-\bar{N}_{\Delta Ty}\right)\Bigg]f(\tau)+\frac{1}{32}\frac{\pi^4}{16}\left\{\frac{1}{2}\left(1+\frac{1}{\lambda^4}\frac{E_1}{E_2}\right)-\frac{E_1}{E_2\nu_{12}\Delta}\frac{1}{\lambda^2}\left(1+\frac{E_1}{E_2\nu_{12}}\frac{1}{\lambda^2}\right)-\frac{E_1}{E_2\nu_{12}\Delta}\frac{1}{\lambda^2}\left(1+\frac{\lambda^2}{\nu_{12}}\right)\right\}\cdot$$

$$f^3(\tau)=\frac{4}{\pi^4}\bar{q}\cos\omega t \tag{35}$$

where $\Delta=1-\dfrac{1}{\nu_{12}^2}\dfrac{E_1}{E_2}$.

2.4 The recovery stress of the constrained SMA fibers

Based on the one-dimensional model of SMA proposed by Brinson[9] and assuming all SMA fibers are fully constrained, we can get the following expressions for the recovery stress of SMA

$$\sigma_r=\begin{cases}\sigma_0+\Theta(T-T_0) & 0\leqslant T\leqslant A_s^\sigma\\ \sigma_1+\left[E_s(\xi)-E_s(\xi_0)\right]\varepsilon_0+\Omega(\xi)\xi_s- & \\ \Omega(\xi_0)\xi_{s0}+\Theta(T-A_s^\sigma) & A_s^\sigma\leqslant T\leqslant A_f^\sigma\\ \sigma_2+\Theta(T-A_f^\sigma) & T\geqslant A_f^\sigma\end{cases} \tag{36}$$

where ξ denotes the Martensite fraction; $E_s(\xi)$ denotes the elastic modulus of SMA, Θ represents the thermal elastic modulus, T represents temperature and T_0 is the reference temperature, the subscript 0 denotes initial conditions, A_s^σ and A_f^σ denote the start and finish temperatures of Austenite under stress, ξ_s is the Martensite fraction induced by stress. The first expression in Eq.(36) is used for SMA in the initial Martensite state, while the third expression is used for SMA in 100% Austenite state, and the second one is used for SMA in the phase transformation state from Martensite to Austenite.

The phase transformation coefficient $\Omega(\xi)$ and the elastic modulus $E_s(\xi)$ can be expressed respectively as

$$\left.\begin{aligned}\Omega(\xi)&=-\varepsilon_L E_s(\xi)\\ E_s(\xi)&=E_A+\xi(E_M-E_A)\end{aligned}\right\} \tag{37}$$

The Austenite start temperature A_s^σ and finish temperature A_f^σ under stress have the following expressions

$$\left.\begin{aligned}A_s^\sigma&=\frac{a_A A_s+b_A(\Theta T_0-\sigma_0)}{a_A+b_A\Theta}\\ A_f^\sigma&=\left\{a_A A_s+\pi-b_A\{[E_A-E(\xi_0)]\varepsilon_0-\Omega(\xi_0)\xi_{s0}+\sigma_0-\Theta T_0\}\right\}/(a_A+b_A\Theta)\end{aligned}\right\} \tag{38}$$

The two constants in Eq.(36) are

$$\left.\begin{aligned}\sigma_1&=\sigma_0+\Theta(A_s^\sigma-T_0)\\ \sigma_2&=\sigma_1+\left[E_A-E_s(\xi_0)\right]\varepsilon_0-\Omega(\xi_0)\xi_{s0}+\Theta(A_f^\sigma-A_s^\sigma)\end{aligned}\right\} \tag{39}$$

The dynamic equations of SMA transformed from Martensite to Austenite are

$$\left.\begin{aligned}\xi&=\frac{\xi_0}{2}\left\{\cos\left[a_A(T-A_s-\frac{\sigma_r}{C_A})\right]+1\right\}\\ \xi_s&=\xi_{s0}-\frac{\xi_{s0}}{\xi_0}(\xi_0-\xi)\\ \xi_T&=\xi_{T0}-\frac{\xi_{T0}}{\xi_0}(\xi_0-\xi)\\ \xi_0&=\xi_{s0}+\xi_{T0}\\ a_A&=\frac{\pi}{A_f-A_s},b_A=-\frac{a_A}{C_A}\\ a_M&=\frac{\pi}{M_s-M_f},b_M=-\frac{a_M}{C_M}\end{aligned}\right\} \tag{40}$$

where M_s, M_f, A_s and A_f denote the Martensite start, Martensite finish, Austenite start and Austenite finish temperatures respectively, ξ_T denotes the Martensite fraction induced by temperature, C_M and C_A are phase transformation constants.

3 Numerical Results and Discussions

Using HBM, the natural frequency equation and the steady-state frequency-response equation in forced vibration of the system are obtained as follows:

$$\frac{\omega_N^2}{\omega_L^2}=1+\frac{3}{4}\frac{K_N}{K_L}\tilde{A}_1^2 \tag{41}$$

$$(K_L-\omega^2)\tilde{A}_2+\frac{3}{4}K_N A^3=\frac{4}{\pi^4}\bar{q} \tag{42}$$

where

$$K_L=\frac{1}{4}\Bigg[\left(\frac{\pi}{2}\right)^4\frac{1}{\lambda^4}\frac{E_1}{12\mu E_2}+2\left(\frac{\pi}{2}\right)^4\frac{1}{\lambda^2}\left(\frac{\nu_{12}}{12\mu}+\frac{1}{6}\frac{G_{12}}{E_2}\right)+\left(\frac{\pi}{2}\right)^4\frac{1}{12\mu}+\left(\frac{\pi}{2}\right)^2\frac{1}{\lambda^2}\left(\bar{N}_{rx}-\bar{N}_{\Delta Tx}\right)+\left(\frac{\pi}{2}\right)^2\left(\bar{N}_{ry}-\bar{N}_{\Delta Ty}\right)\Bigg]$$

$$K_{\mathrm{N}}=\frac{1}{32}\frac{\pi^4}{16}\left\{\frac{1}{2}\left(1+\frac{1}{\lambda^4}\frac{E_1}{E_2}\right)-\frac{E_1}{E_2\nu_{12}\Delta}\frac{1}{\lambda^2}\cdot\left(1+\frac{E_1}{E_2\nu_{12}}\frac{1}{\lambda^2}\right)-\frac{E_1}{E_2\nu_{12}\Delta}\frac{1}{\lambda^2}\left(1+\frac{\lambda^2}{\nu_{12}}\right)\right\} \quad (43)$$

where $\tilde{A}_1$, $\tilde{A}_2$ are the free and forced vibration amplitude respectively, ω_{L} and ω_{N} are linear and nonlinear natural frequencies respectively, ω is excited frequency.

In the present work the symmetric NiTi/graphite/epoxy laminate $[0/90/0/90/0]_{\mathrm{s}}$ with the thickness $h=0.002$ m is used for simulation, where the thickness of each layer is $h_k=0.002/10$ m ($k=1, 2, \cdots, 10$). The material parameters used in this simulation are given below.

(1) Graphite/epoxy[12]

$E_{1\mathrm{m}}=155(1-3.53\times10^{-4}\Delta T)$ GPa

$E_{2\mathrm{m}}=8.07(1-4.27\times10^{-4}\Delta T)$ GPa

$G_{12\mathrm{m}}=4.55(1-6.06\times10^{-4}\Delta T)$ GPa

$\rho_{\mathrm{m}}=1\,586\ \mathrm{kg/m^3}$

$\alpha_{1\mathrm{m}}=-0.07\times10^{-6}(1-1.25\times10^{-3}\Delta T)$ (1/° C)

$\alpha_{2\mathrm{m}}=30.1\times10^{-6}(1+0.41\times10^{-4}\Delta T)$ (1/° C)

$\Delta T=T-T_{\mathrm{ref}}$, $T_{\mathrm{ref}}=20$ °C, $\nu_{12\mathrm{m}}=0.22$

(2) SMA fibers

$E_{\mathrm{A}}=67$ GPa, $E_{\mathrm{M}}=26.3$ GPa, $M_{\mathrm{s}}=18.4$ °C

$M_{\mathrm{f}}=9$ °C, $A_{\mathrm{s}}=34.5$ °C, $A_{\mathrm{f}}=49$ °C

$C_{\mathrm{M}}=8$ MPa/° C, $C_{\mathrm{A}}=13.8$ MPa/° C, $\Theta=0.55$

$\varepsilon_{\mathrm{L}}=0.067$, $\sigma_0=0$, $T_0=20$ °C, $\xi_{\mathrm{s}0}=0.075$

$\xi_{\mathrm{T}0}=0$, $\varepsilon_0=0.05$, $\nu_{\mathrm{s}}=0.33$, $\rho_{\mathrm{s}}=6\,450\ \mathrm{kg/m^3}$

$\alpha_{\mathrm{s}}=10.26\times10^{-6}$ (1/° C)

The simulation results are shown in the following figures. Fig.1 gives the free-vibration frequency ratio of the NiTi/graphite/epoxy symmetric laminate varying with temperature, where $\lambda=0.5$, $b/h=10$, $V_{\mathrm{s}}=0.4$ and $\tilde{A}_1=1.0$. It can be seen that the natural frequency of the nonlinear laminate is larger than that of the linear one due to the increased in-plane stiffness and the frequency ratio of the nonlinear laminate to the linear one shows ascending, descending and then ascending trend with the increasing of temperature. This situation results from the variation of the recovery stress of the fully constrained NiTi fibers in the laminate. When temperature is between 0 and 20 °C, as NiTi fibers are not actuated, the recovery stress σ_{r} is zero. But the in-plane compressive forces induced by temperature exist in the laminate, which results in the descending of ω_{L} as temperature is increasing; When temperature lies within the range of 20 °C and A_{s}^{σ}, ω_{L}, still decreases with the increasing of temperature. Though NiTi fibers are actuated in this temperature range, yet new Austenite has not produced and σ_{r} is very small. The laminate is still in in-plane compression; When temperature is between A_{s}^{σ} and A_{f}^{σ}, σ_{r} increases obviously with the increasing of temperature due to the phase transformation from Martensite to Austenite and the total in-plane forces of the laminate become tensile, so ω_{L} increases obviously with the increasing of temperature; When temperature is higher than A_{f}^{σ}, the curve shows the same trend as that in the temperature range of 20 °C and A_{s}^{σ}. Because Martensite in NiTi fibers are fully transformed into Austenite and the in-plane forces induced by temperature become dominant forces again that lead to the total compressive in-plane forces in the laminate.

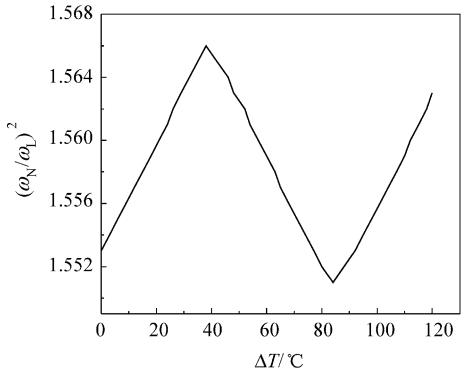

Fig.1 The free-vibration frequency ratio of NiTi/graphite/epoxy symmetric laminate varying with temperature. ($\lambda=0.5$, $b/h=10$, $V_{\mathrm{s}}=0.4$, $\tilde{A}_1=1.0$)

It should be pointed out that ω_{L} is existing in the denominator of Eq.(41), so it shows an opposite trend with that of σ_{r} as shown in Fig.1.

Fig.2(a) shows the free-vibration frequency ratio varying with temperature for NiTi/ raphite/epoxy laminates with two non-dimensional vibration amplitudes. We can see that the smaller the non-dimensional vibration amplitude is, the flatter the

curve becomes.

The effects of volume fractions of NiTi on the free-vibration frequency ratio are shown in Fig.2(b). From this figure we can see that the volume fraction of NiTi can improve the free-vibration frequency ratio. And the higher the volume fraction of NiTi is, the more wide the curve varying range is. This figure also demonstrates that the natural frequency of the linear laminate becomes more and more obvious with the increase of volume fractions of NiTi, which means that the less effects of the geometric nonlinearity of the laminate will be when the volume fraction of NiTi fibers is higher.

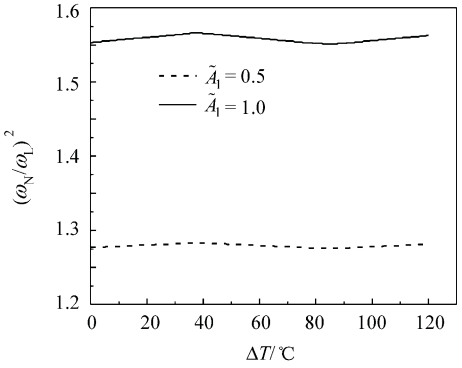

(a) The effects of non-dimensional vibration range $\tilde{A}_1$

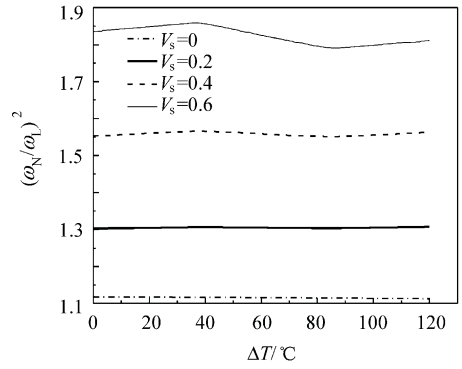

(b) The effects of volume fractions of TiNi fibers V_s

Fig.2 The free-vibration frequency ratio of NiTi/graphite/epoxy symmetric laminate varies with temperature. (λ=0.5, b/h=10)

Under forced vibration, the steady-state frequency responses of the laminate embedded with NiTi fibers in 100% Austenite, initial 100% Martensite and phase transformation from Martensite to Austenite states are shown in Fig.3, Fig.4 and Fig.5 respectively. In each figure, three amplitudes of the excitation forces with $\bar{q}=5$, $\bar{q}=20$ and $\bar{q}=50$ are considered to observe their effects on the frequency responses. It can be seen that the temperature nearly has no effects on the shapes of the frequency-response curves, but it has certain effects on the positions of the framework curves, that is the framework curves shift rightwards with the increasing of temperature. Among the three typical cases, the framework curves will shift rightwards with the largest range when NiTi fibers are in the phase transformation state from Martensite to Austenite. This is due to the large increase of σ_r and results in the large increase of the in-plane stiffness, which corresponds to the conclusion derived from Fig.1.

The frequency-response curves of the NiTi hybrid laminate are shown in Fig.6 with the aspect ratio of λ=0.25, λ=0.50 and λ=1.00. It can be seen that the frequency-response curves are sensitive to the aspect ratio λ. The framework curve of the frequency-response curves will shift leftwards with a large range when λ is increased while the vibration amplitudes are also increased obviously.

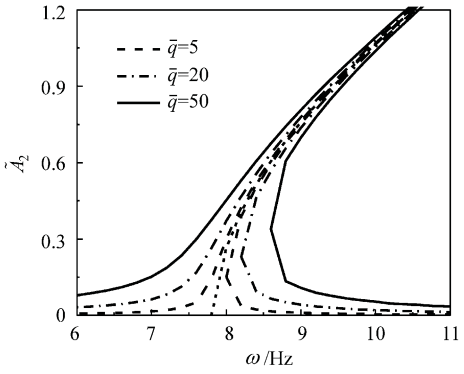

Fig.3 Frequency responses of the laminate embedded with 100%-Austenite NiTi fibers under the excitations with different amplitudes. (T=100 ℃, λ=0.5, V_s=0.4)

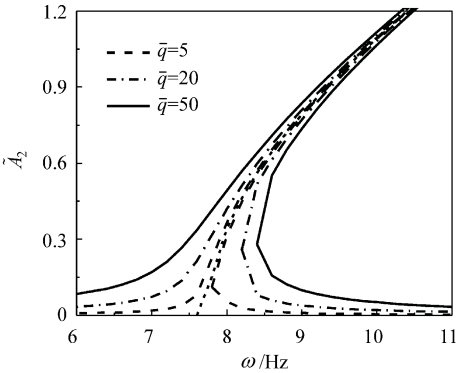

Fig.4 Frequency responses of the laminate embedded with initial 100%-Martensite NiTi fibers under the excitations with different amplitudes. (T=30℃, λ=0.5, V_s=0.4)

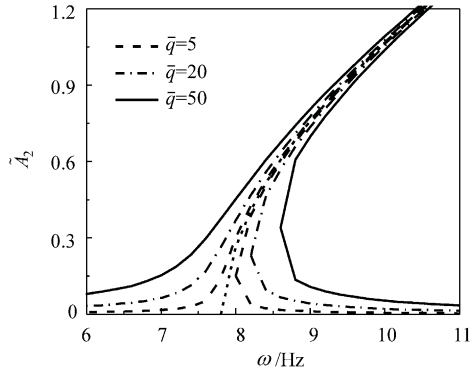

Fig.5 Frequency responses of the laminate embedded with NiTi fibers in the phase transformation state from Martensite to Austenite under the excitations with different amplitudes. (T=70℃, λ=0.5, V_s=0.4)

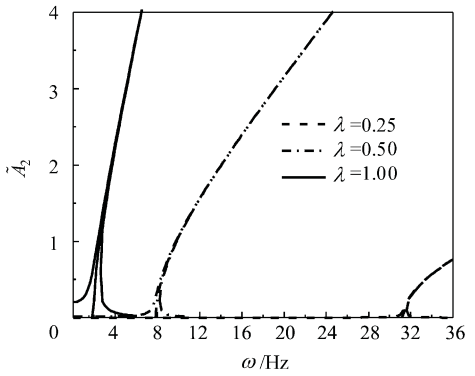

Fig.6 Frequency responses of the laminate embedded with 100%-Austenite NiTi fibers at three different aspect ratios λ. (T=100℃, V_s=0.4, $\bar{q}=20$)

4 Conclusions

Based on the nonlinear theory of the symmetric orthotropic elastic laminates and the Brinson's SMA model, the natural frequency equation under free vibration and the steady-state frequency-response equation under forced vibration are established for the SMA reinforced composite laminates with large deflections by using the Galerkin approximate method and HBM. The following conclusions can be drawn:

(1) The trend of the frequency ratio of NiTi/graphite/epoxy symmetric laminate under nonlinear free vibration varies with temperature is similar to that of the recovery stresses of fully constrained NiTi fibers when actuated. And this behavior becomes more obvious when the volume fraction of NiTi fibers is higher.

(2) At the same actuation temperature, the frequency ratio of the laminate under nonlinear free vibration increases with the increasing of volume fractions of NiTi fibers and the non-dimensional vibration amplitudes.

(3) Under the forced vibration, the framework curve of the frequency-response curves of the laminate will shift rightwards with the largest range when NiTi fibers are in the phase transformation state from Martensite to Austenite due to the corresponding largest in-plane stiffness.

(4) The aspect ratio λ of the laminate has a dramatic effect of the frequency-response curves. The framework curve of the frequency-response curves will shift leftwards with a large range and the vibration range will also be increased obviously.

References

[1] Birman V. Review of mechanics of shape memory alloy structures. Appl Mech Rev 1997; 50: 629-645.

[2] Ren Yongsheng. Progress of SMA intelligent composites. Journal of Composite Materials 1999; 16(1): 1-7. [in Chinese]

[3] Chu L C. Integrated intelligent structures for suppressing static aerothermoelastic deformations and flutter of panels. AFOSR-TR-950053, 1995.

[4] Zou Jing. The constitutive relation of shape memory alloy and the analysis by the finite element method of shape memory alloy reinforced composite laminated plates. PhD thesis, Huazhong University of Science and Technology; 1999. [in Chinese]

[5] Dano M L, Hyer M W. SMA-induced snap-through of unsymmetric fiber-reinforced composite laminates. Int J Solids and Structures 2003; 40: 5949-5972.

[6] Park J S, Kim J H, Moon S H. Vibration of thermally post-buckled composite plates embedded with shape memory alloy fibers. Composite Structures 2004; 63: 179-188.

[7] Park J S, Kim J H, Moon S H. Thermal post-buckling and flutter characteristics of composite plates embedded with shape memory alloy fibers. Composites: Part B 2005; 36: 627-636.

[8] Cho M, Kim S. Structural morphing using two-way shape memory effect of SMA . Journal of Solids and Structures 2005; 42: 1759-1776.

[9] Brinson L C. One-dimensional thermomechanical constitutive relations for shape memory alloy: thermomechanical derivation with non-costant material functions and redefined martensite internal variable. J Intelli Mater Syst and Struct 1993; 4: 229-242.

[10] Zhong Z W, Chen R R, Mei C. Buckling and postbuckling of shape memory alloy fiber-reinforced composite plates. In: Noor A K, editor. Buckling and postbuckling of composite structures. New York: ASME, 1994; 115-132.

[11] Zhong Z W, Mei C. Finite element vibration analysis of composite plates with embedded shape memory alloy fibers at elevated temperatures. Design Engineering Technical Conference. New York: ASME, 1984(3): 675-684.

[12] Duan B, Taw K M, Goek S, et al. Analysis and control of large thermal defection of composite plates using shape memory alloy. SPIE_s 7th International Symposium on Smart Structures and Materials. Newport Beach, CA, 2000(3991): 358-365.

Biographies:

Ren Yongsheng Born in 1956, he received B.S. and M.S. from Taiyuan University of Technology in 1982 and from Southeast University in 1989 respectively. He received his Ph.D. from Nanjing University of Aeronautics and Astronautics in 1992. He is currently a professor in College of Mechanical and Electronic Engineering, Shandong University of Science and Technology. His research interests include nonlinear dynamics, smart materials, vibration and shock control and aeroelasticity, etc. He has published several scientific papers in different periodicals.

E-mail: renys@sdust.edu.cn

Sun Shuangshuang Born in 1971, she received B.S. and M.S. from Qingdao University of Science and Technology in 1996 and 1999 respectively. She received her Ph.D. from Shanghai Jiaotong University in 2003. She is currently an associate professor in College of Electro-mechanical Engineering, Qingdao University of Science and Technology. Her research interests include nonlinear dynamics and smart materials.

E-mail: sunkira@sohu.com

Appendix A: The Elastic Constants of NiTi Fiber Hybrid Composites

The elastic constants are calculated according to the following mixture theory[11]

$$E_1 = E_{1\mathrm{m}}(1-V_\mathrm{s}) + E_\mathrm{s}V_\mathrm{s},\ \ E_2 = \frac{E_{2\mathrm{m}}E_\mathrm{s}}{E_{2\mathrm{m}}V_\mathrm{s} + E_\mathrm{s}(1-V_\mathrm{s})}$$

$$G_{12} = \frac{G_{12\mathrm{m}}G_\mathrm{s}}{G_{12\mathrm{m}}V_\mathrm{s} + G_\mathrm{s}(1-V_\mathrm{s})},\ \nu_{12} = \nu_{12\mathrm{m}}(1-V_\mathrm{s}) + \nu_\mathrm{s}V_\mathrm{s}$$

$$G_\mathrm{s} = \frac{E_\mathrm{s}}{2(1+\nu_\mathrm{s})},\ \alpha_1 = \frac{E_{1\mathrm{m}}\alpha_{1\mathrm{m}}(1-V_\mathrm{s}) + E_\mathrm{s}\alpha_\mathrm{s}V_\mathrm{s}}{E_1}$$

$$\alpha_2 = \alpha_{2\mathrm{m}}(1-V_\mathrm{s}) + \alpha_\mathrm{s}V_\mathrm{s}$$

$$m_0 = \sum_{i=1}^{N}\left[\rho_\mathrm{m}(1-V_\mathrm{s}) + \rho_\mathrm{s}V_\mathrm{s}\right](z_k - z_{k-1})$$

where the subscript m denotes the composite medium, and the subscript s denotes SMA. E, G and ν denote the tension-compression elastic modulus, the shearing elastic modulus and the possion ratio respectively. α and ρ denote thermal expansion coefficient and density respectively. V denotes the volume percentage.